3D Face Recognition Founded on the Structural Diversity of Human Faces

Shalini Gupta[1], J. K. Aggarwal[1], Mia K. Markey[2], Alan C. Bovik[1]
[1]The Department of Electrical and Computer Engineering,
The University of Texas at Austin, TX 78712, USA
[2]The University of Texas Department of Biomedical Engineering, Austin, TX 78712, USA
{shalinig@ece, aggarwaljk@mail, mia.markey@mail, bovik@ece}.utexas.edu

Abstract

We present a systematic procedure for selecting facial fiducial points associated with diverse structural characteristics of a human face. We identify such characteristics from the existing literature on anthropometric facial proportions. We also present three dimensional (3D) face recognition algorithms, which employ Euclidean/geodesic distances between these anthropometric fiducial points as features along with linear discriminant analysis classifiers. Furthermore, we show that in our algorithms, when anthropometric distances are replaced by distances between arbitrary regularly spaced facial points, their performances decrease substantially. This demonstrates that incorporating domain specific knowledge about the structural diversity of human faces significantly improves the performance of 3D human face recognition algorithms.

1. Introduction

Automated person identification is a problem of considerable practical significance. It has numerous applications including automated screening, surveillance, authentication, and human computer interaction. Considerable progress has been made in the area of two dimensional (2D) face recognition in which intensity/color images of human faces are employed. However, 2D systems are reported to perform poorly when variations in facial pose, ambient illumination, or facial expression are present [20].

Recently, research attention is being directed towards developing algorithms for three dimensional (3D) face recognition [11]. For such techniques, 3D facial models are either explicitly captured using 3D image acquisition devices or are synthetically generated from 2D images using morphing techniques. The 3D shape of a face depends on its anatomical structure and is independent of its pose which can be corrected by rigid rotations in 3D space [17]. Furthermore, when 3D facial models are acquired using active devices (*e.g.*, laser range finders), they are not affected by ambient illumination conditions during image acquisition.

A few techniques for 3D face recognition that are based on geometric properties of local facial landmarks/fiducial points, and Euclidean distances, ratios of distances, or angles between them have been developed [9, 18, 15, 23, 14]. However, in none of these analyses has the choice of local facial geometric features been founded on a fundamental understanding of discriminatory structural characteristics of the human face.

In this paper, we present a novel systematic procedure for selecting facial fiducial points associated with diverse structural characteristics of a human face. We identify such characteristics from the existing literature on anthropometric facial proportions [6]. We also present novel effective face recognition algorithms, which employ Euclidean/geodesic distances between these anthropometric fiducial points as features along with linear discriminant analysis (LDA) classifiers.

Previously, we had demonstrated the superior performance of similar algorithms over the 3D 'eigensurfaces' and 3D 'fishersurfaces' approaches [10]. In this paper, we further demonstrate how the choice of facial fiducial points critically effects the performance of 3D face recognition algorithms that employ distances between them as features. Specifically, we show that in our proposed algorithms, when anthropometric facial distances are replaced by distances between arbitrary regularly spaced facial points, their equal error rates (EER) decrease by nearly an order of magnitude and rank 1 recognition rates (RR) also decrease significantly.

2. Related work

The majority of existing 3D face recognition algorithms are 'holistic,' in which facial information from entire faces/facial range images is employed. These include statistical techniques *e.g.*, principal component analysis (PCA), LDA, or hidden Markov models that are applied to depth

values of facial range images, and techniques involving iterative rigid alignment and comparison of facial models [11]. Statistical techniques are straight-forward extensions of successful 2D techniques to facial range images where it is not obvious as to what discriminatory facial information is encoded. Facial surface matching techniques, on the other hand, are computationally expensive [17], which limits their practical applicability.

In comparison to 'holistic' techniques, 3D face recognition algorithms based on local geometric facial characteristics are relatively less developed. This is true despite the fact that two out of three of the most successful 2D face recognition techniques at the Face Recognition Vendors Test 2002 [20], were based on local facial features (elastic bunch graph matching (EBGM) [24] and local feature analysis [19]). Furthermore, a combination of 2D EBGM and 3D EBGM (extension of 2D EBGM to facial range images) has resulted in the most successful 2D+3D face recognition technique evaluated on the benchmark Face Recognition Grand Challenge (FRGC) data set [14]. However, in this analysis the authors observed that 2D EBGM significantly outperformed 3D EBGM. They highlighted the need to design local features-based 3D face recognition techniques based on an understanding of discriminatory facial characteristics in order to realize their potential.

Other notable 3D techniques based on local facial features are those by Gordon [9] and Moreno *et al*. [18], in which the authors employed surface areas and curvatures of facial landmarks, and distances and angles between them with a nearest neighbor classifier. Lee *et al*. [15] reported a technique where positions, distances, ratios of distances, and angles between 8 fiducial points were employed as features with a support vector machine classifier. Wang *et al*. [23] employed 'point signatures' at four fiducial points as features. This technique was found to be robust to variations in facial pose and expression.

Pattern recognition techniques based on local features of objects are known to be less affected by global variations including noise, occlusions, and rotations [1, 16]. For the task of face recognition, such techniques present a further advantage that the choice of local facial features can be guided by domain specific knowledge about the structural diversity of human faces. However, in all existing 3D algorithms based on local facial features, such an approach has not been adopted for selecting facial landmarks. Rather, the choice of landmarks has either been arbitrary [9, 18, 15, 23] or an extension of 2D local features-based techniques [14]. In comparison to 2D facial images that provide information about facial texture, 3D facial models provide rich information about facial structure, making the 3D face recognition problem fundamentally different from the 2D problem. This may explain why Hüsken *et al*. [14] observed better performance for 2D EBGM than for 3D EBGM.

Hence, it is to our advantage to identify and exploit discriminatory facial structural information to design effective 3D face recognition algorithms. In this paper, we address this issue and present a technique for systematically identifying discriminatory facial measurements between specific facial fiducial points from the existing literature on anthropometric facial proportions. We present effective 3D face recognition algorithms that employ these measurements. Furthermore, we demonstrate how our proposed selection of anthropometric fiducial points results in significantly superior performance relative to algorithms that employ facial measurements between arbitrary facial fiducial points.

3. Methodology

3.1. Fiducial points selection

Our first novel contribution is the identification of discriminatory facial structural characteristics from the existing literature on anthropometric facial proportions. Anthropometry is the branch of science that deals with the quantitative description of physical characteristics of the human body. Anthropometric cranio-facial proportions are ratios of pairs of straight-line and/or along-the-surface distances between specific cranial and facial fiducial points [6]. For example, the most commonly used nasal index $N1$ is the ratio of the horizontal nose width to the vertical nose height ($N1 = (al - al)/(n - sn)$ from Figure 1(b)). Intuitively, anthropometric facial proportions quantify relationships between different sub-parts of the human face. The science of physical facial anthropometry has existed for nearly three centuries, over the course of which researchers have have proposed, measured, recorded, and employed numerous anthropometric proportions for various tasks.

Cranio-facial proportions are widely employed in art and sculpture as guiding canons for creating well-proportioned ideal faces, in anthropology for analyzing prehistoric human remains [3], for quantifying facial attractiveness [8], for analyzing facial disproportionality in anomalies or after injury as an aid to planning facial cosmetic and reconstructive surgery [6, 21], and recently for creating parametric models of human faces in computer graphics [4]. As far back as 1939, Hrdlička emphasized the importance of anthropometric facial proportions for comparing groups of people or populations [13]. However, they have not been employed for designing 3D face recognition algorithms.

After extensively examining prior literature on physical anthropometry, Farkas consolidated a list of 129 of the most basic cranio-facial anthropometric proportions that had been employed for various tasks [6]. She also recorded their average and standard deviation (σ) values by collecting physical measurements for 1312 adult human subjects belonging to diverse ethnic, gender, and age groups [6, 7]. From among these, we identified 70 anthropometric propor-

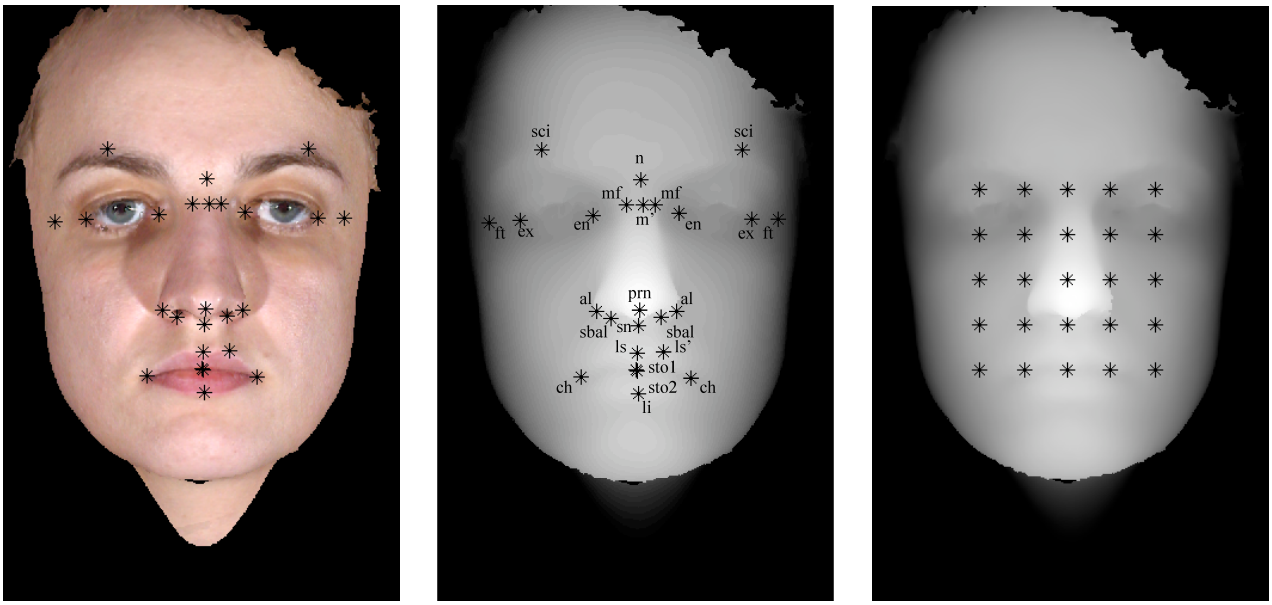

(a) (b) (c)

Figure 1. The figure depicts (a) 25 anthropometric fiducial points on a texture image; (b) 25 anthropometric fiducial points on a range image; (c) 25 arbitrary equally spaced points overlaid on the main facial features.

tions that can be reliably calculated by locating appropriate facial fiducial points on facial models normally acquired using 3D devices.

From among these 70 facial proportions, we selected a third (23) of the most variable anthropometric facial proportions (with the highest standard deviation values presented in Table 1) as being representative of discriminatory facial structural characteristics. We reasoned that characteristics that display wide variation between individuals are likely to be most useful for distinguishing them. This information forms the basis of our proposed 3D face recognition algorithms.

We manually located 25 anthropometric facial fiducial points (Figure 1(a)) associated with these 23 most variable anthropometric proportions (Table 1) on the color image of each the 1128 facial models in our data set. Since we employed a stereo imaging system to acquire facial data, pairs of facial color and range images of each subject were perfectly aligned. Hence, the corresponding locations of fiducial points on range images were automatically obtained (Figure 1(b)).

For this intermediary analysis, which was designed to evaluate the potential and feasibility of our proposed face recognition algorithm based on anthropometric facial measurements, we located the fiducial points manually. We reasoned that only upon establishing the feasibility of our technique, would it be worthwhile to develop algorithms to automatically locate these fiducial points, which will be our next step towards building a fully automatic system.

3.2. Feature extraction and classification

For all algorithms presented in this paper, we employed features calculated from facial range images only. We employed (a) 300 3D Euclidean distances, and (b) 300 geodesic distances between all pairs of the 25 anthropometric facial fiducial points (Figure 1(b)) as features for two 3D face recognition algorithms: EUC_{ANT} and GEO_{ANT}, respectively. We calculated geodesics using the Dijkstra's shortest path algorithm by defining 8 connected nearest neighbors about each point [5, 22].

We investigated geodesic distances as they have not been employed previously for local features-based 3D face recognition algorithms. Geodesics are known to perform better than Euclidean distances at representing 'free form' surfaces [12]. Furthermore, a recent study suggested that changes in facial expressions may be modeled as isometric deformations of the facial surface [2], under which intrinsic properties including geodesics of a surface remain constant. Hence, algorithms based on geodesic distances are likely to be robust to changes in facial expressions.

For both the EUC_{ANT} and GEO_{ANT} algorithms, we individually selected subsets of the most discriminatory distance features using stepwise linear discriminant analysis ('stepdisc', SAS Institute Inc., NC, USA) and reduced each subset of features further to 11 dimensional (11D) spaces using Fisher's LDA. These steps were applied only to a training data set and all images in the test data set were projected onto the learned LDA directions. We calculated the

S. No	Anthropometric Proportion	σ
1.	$O3 = \frac{(ex-en,l)}{(en-en)}$	7.75
2.	$O10 = \frac{(en-en)}{(al-al)}$	8.26
3.	$O12 = \frac{(en-en)}{(ch-ch)}$	6.02
4.	$F32 = \frac{(n-sto1)}{(ex-ex)}$	5.30
5.	$N1 = \frac{(al-al)}{(n-sn)}$	5.81
6.	$N2 = \frac{(mf-mf)}{(al-al)}$	7.08
7.	$N4 = \frac{(sbal-sn,l+r)}{(al-al)}$	8.80
8.	$N6 = \frac{(ex-m'_{sag},l)}{(mf-mf)}$	14.6
9.	$N7 = \frac{(sn-prn)}{(al-al)}$	6.28
10.	$N8 = \frac{(sn-prn)}{(sbal-sn,l+r)}$	12.8
11.	$N15 = \frac{(en-m'_{sag},l)}{(sn-prn)}$	11.2
12.	$N16 = \frac{(en-m'_{sag},l)}{(en-m,l)}$	7.26
13.	$N30 = \frac{(mf-mf)}{(en-en)}$	6.06
14.	$N31 = \frac{(ex-m'_{sag},l)}{(en-en)}$	7.01
15.	$N32 = \frac{(al-al)}{(ch-ch)}$	5.04
16.	$N33 = \frac{(sn-prn)}{(sn-sto1)}$	13.8
17.	$L1 = \frac{(sn-sto1)}{(ch-ch)}$	5.40
18.	$L4 = \frac{(sn-ls)}{(sbal-ls',l)}$	10.2
19.	$L5 = \frac{(sn-ls)}{(sn-sto1)}$	5.97
20.	$L6 = \frac{(ls-sto1)}{(sn-sto1)}$	7.10
21.	$L7 = \frac{(ls-sto1)}{(sn-ls)}$	13.3
22.	$L9 = \frac{(ls-sto1)}{(sto2-li)}$	16.9
23.	$L14 = \frac{(sn-sto1)}{(n-sn)}$	5.10

Table 1. The table presents the 23 most variable anthropometric facial proportions along with their standard deviation (σ) values for adult humans reported by Farkas [6]. The corresponding fiducial points are depicted in Figure 1(b). Nasal proportion are denoted by N, orbital proportions by O, facial proportions by F, and L denotes proportions associated with the lips and mouth region.

final distance between faces in the 11D LDA space using the Euclidean distance metric.

3.3. Effect of facial fiducial points

We also investigated the effect of the selection of facial fiducial points on the performance of our proposed 3D face recognition algorithms. We repeated the two algorithms with Euclidean and geodesic distances between arbitrary facial points placed along a regularly spaced rectangular grid overlaid on the primary facial features (Figure 1(c)), instead of distances between anthropometric fiducial points (Figure 1(b)). We denote these algorithms by EUC_{ABR} and GEO_{ABR}, respectively. The grid points were always located in the range image region between left and right coordinates of 80 and 420, respectively, and upper and lower coordinates 173 and 526, respectively. For the facial range images that we employed, these limits enclosed the central region of all faces. This choice of arbitrary facial points was motivated by the fact that they capture distances between the significant facial landmarks (the eyes, nose and the mouth regions) without requiring localization of specific facial fiducial points and have been employed in previous 3D face recognition algorithms [17].

3.4. Performance evaluation

We employed a data set, which contained 1128 3D facial models of 105 subjects. Shape and texture data for each face was acquired using an MU-2 stereo imaging system manufactured by 3Q Technologies Ltd. (Atlanta, GA). The data contained neutral and smiling faces with/without open mouths. All subjects were requested to remove hats and eye-glasses.

All 3D facial models were normalized to a canonical frontal pose by iteratively registering them to a template face in that orientation. A pair of 3D range and color images for each pose normalized face were constructed (Figures 1(a) and 1(b)). Hence at each (x, y) location of a face, a depth (z) value and a set of (r, g, b) values was available. The facial range images were of size 715×501 pixels and had a resolution of 0.32 mm along the x, y and z dimensions (courtesy Advanced Digital Imaging Research, LLC, Friendswood, TX). We median filtered the range images to remove impulse noise, filled holes by a process of bicubic interpolation and low pass filtered them using a Gaussian kernel of size 7×7 pixels and $\sigma = 1$.

The data was randomly partitioned into a training set containing 360 range images of 12 subjects (30 images per subject) in neutral or expressive modes, and a test set containing the remaining images. All the steps involved in feature selection and classifier training were performed using only the training data and were applied to data in the independent test set. The test set was further randomly partitioned into a gallery set and a probe set. Consistent with

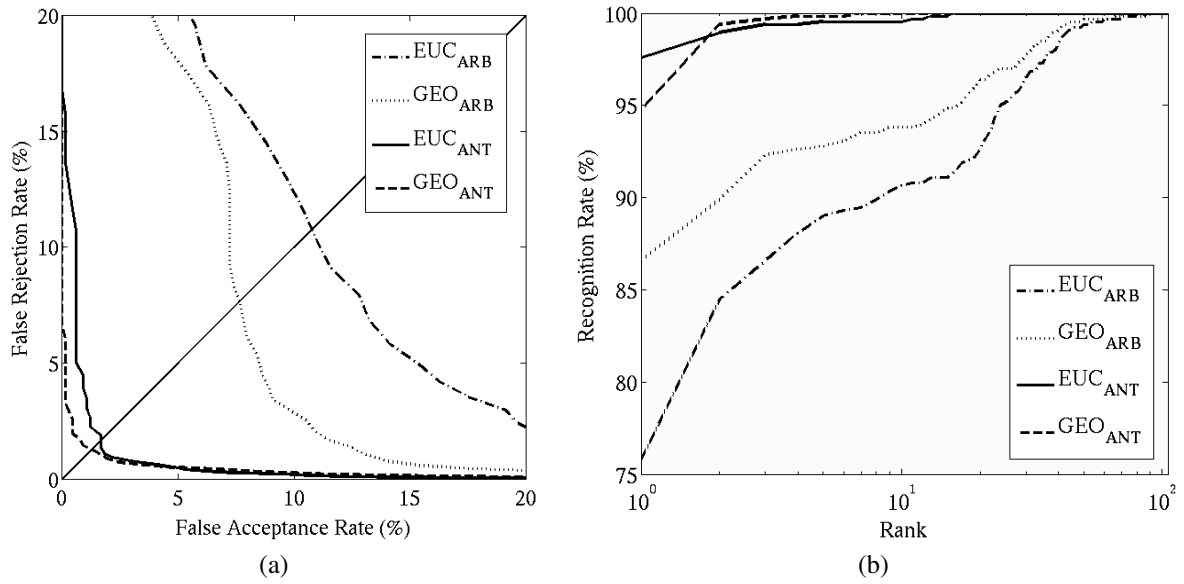

Figure 2. The figure presents (a) ROC curves for the verification performance, and (b) semi-logarithmic plots of the CMC curves for the identification performance of 3D face recognition algorithms, for all probe images.

the established face recognition evaluation protocols [20], the gallery set contained one image each of 105 subjects with a neutral facial expression. The probe set contained another 663 images of the gallery subjects with a neutral or a smiling (with/without open mouth) facial expression. In the probe set, the number of range images of each subject varied from 1 to 55.

We evaluated the performance of the four 3D face recognition algorithms separately for the entire probe set, for neutral probes only, and for expressive probes only. Verification performance was evaluated using receiver operating characteristic (ROC) curve methodology and EER values and areas under the ROC curves (AUC) were noted. Identification performance was evaluated using cumulative match characteristic (CMC) curves and the rank 1 RR values were observed. Statistical 95% confidence intervals for the EER, AUC, and the rank one RR values were obtained empirically by bootstrap sampling.

4. Results

Tables 2 and 3 present the EER and the AUC values for the verification performance of the four 3D face recognition algorithms that we implemented. The corresponding ROC curves are presented in Figure 2(a). Rank 1 RR values are presented in Table 4 and the CMC curves are depicted in Figure 2(b). Error bars for the 95% confidence intervals of each observed quantity are also presented in the tables.

Both the proposed algorithms EUC_{ANT} and GEO_{ANT} that employed anthropometric facial distances, performed well with observed EER values of 1.6% and 1.3%, respectively, and rank 1 RR values of 97.6% and 94.7%, respectively. GEO_{ANT} was more robust to variable facial expressions than EUC_{ANT} at the task of verifying faces. This can be inferred from the fact that the difference between the AUC and EER values of neutral and expressive probes for GEO_{ANT}, was less than that for EUC_{ANT} (Tables 2 and 3).

Overall, both the algorithms that employed anthropometric facial distances performed significantly better than the corresponding algorithms that employed distances between arbitrary regularly spaced facial points. The EER values for EUC_{ANT} and GEO_{ANT} were nearly 85% lower, and their AUC values were nearly 95% lower than the corresponding values for EUC_{ARB} and GEO_{ARB}, respectively (Tables 2 and 3). The rank 1 RR value for EUC_{ANT} was significantly higher (by 29%) than that for EUC_{ARB}. Similarly, the rank one RR value for GEO_{ANT} was also significantly higher (by 9%) than that for GEO_{ARB} (Table 4).

5. Discussion

In this paper we identified discriminatory facial structural characteristics from the existing literature on anthropometric facial proportions. We hypothesized that facial measurements associated with highly variable anthropometric facial proportions are likely to be useful for distinguishing individuals. In order to investigate further whether this was the case, we separately ranked the anthropometric Euclidean and the geodesic distance features that we employed in the EUC_{ANT} and the GEO_{ANT} algorithms, respectively, in descending order of their individual Fisher's ratio values. The 20 most discriminatory anthropometric Euclidean

	Neutral Probes		Expressive Probes		All Probes	
Algorithm	EER (%)	CI	EER (%)	CI	EER (%)	CI
EUC_{ABR}	11.2	[9.4 13.1]	9.8	[7.2 13.2]	10.6	[9.1 12.5]
GEO_{ABR}	8.5	[6.6 11.3]	5.3	[2.5 7.5]	7.6	[5.9 8.7]
EUC_{ANT}	0.9	[0.7 1.5]	2.9	[1.7 4.0]	1.6	[1.1 2.2]
GEO_{ANT}	1.1	[0.8 1.5]	1.7	[0.7 2.3]	1.3	[0.9 1.7]

Table 2. The observed EER values and their 95% confidence intervals for the verification performance of 3D face recognition algorithms.

	Neutral Probes		Expressive Probes		All Probes	
Algorithm	AUC $\times 10^{-2}$	CI	AUC $\times 10^{-2}$	CI	AUC $\times 10^{-2}$	CI
EUC_{ARB}	3.42	[2.58 4.39]	4.71	[2.82 7.73]	3.81	[3.12 4.79]
GEO_{ARB}	2.29	[1.70 3.04]	2.00	[0.83 3.83]	2.18	[1.58 2.88]
EUC_{ANT}	0.09	[0.05 0.18]	0.32	[0.13 0.65]	0.17	[0.10 0.24]
GEO_{ANT}	0.09	[0.07 0.11]	0.16	[0.10 0.23]	0.12	[0.09 0.15]

Table 3. The observed AUC values and their 95% confidence intervals for the verification performance of 3D face recognition algorithms.

	Neutral Probes		Expressive Probes		All Probes	
Algorithm	RR (%)	CI	RR (%)	CI	RR (%)	CI
EUC_{ARB}	74.4	[70.4 78.4]	79.2	[73.2 85.2]	75.7	[72.6 78.9]
GEO_{ARB}	85.8	[82.6 89.0]	88.5	[83.6 93.2]	86.6	[83.6 89.3]
EUC_{ANT}	97.9	[96.5 99.2]	96.7	[94.0 98.9]	97.6	[96.4 98.6]
GEO_{ANT}	95.2	[93.3 97.1]	93.4	[89.6 96.7]	94.7	[92.9 96.2]

Table 4. The observed rank 1 RR values and their 95% confidence intervals for the identification performance of 3D face recognition algorithms.

and geodesic distance features are depicted in Figure 3. Interestingly, these most discriminatory distance features are predominantly associated with the nasal region of the face as are a majority (12 out of 23) of the anthropometric facial proportions reported to be highly variable for adult humans (Table 1). This observation further substantiates our hypothesis and suggests that identifying highly variable structural characteristics of the human face can be an effective way of discovering discriminatory facial information.

Farkas also identified cranio-facial proportions with significantly different mean values for the two sexes [7] and for different ethnic groups of humans [8]. Interestingly, 17 ($O10$, $O12$, $N1$, $N6$, $N7$, $N8$, $N15$, $N16$, $N30$, $N31$, $N33$, $L1$, $L4$, $L5$, $L6$, $L7$, and $L14$) out of the 23 facial proportions that we selected (Table 1) were also reported to be significantly different for the two sexes by Farkas [7], and one ($N7$) was reported to be significantly different for various ethnic groups of humans [8]. It is very likely that these factors also contribute to the success of our proposed 3D face recognition algorithms based on anthropometric facial distances.

Our proposed 3D face recognition algorithms based on anthropometric facial distances performed significantly better than corresponding algorithms that employed distances between arbitrary facial points (Figure 2). This confirms the fact that 3D face recognition algorithms benefit significantly by incorporating domain specific knowledge about the structural diversity of human faces into their design.

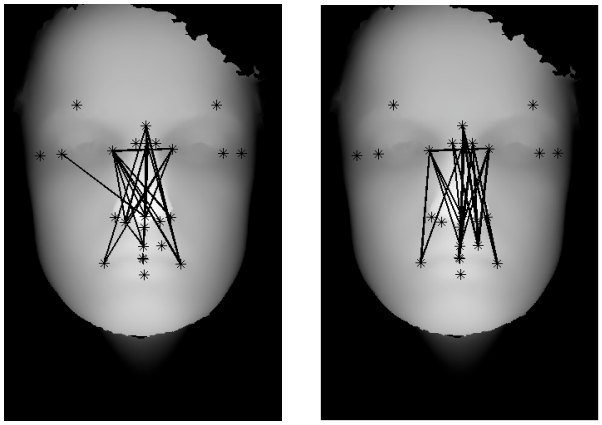

(a) (b)

Figure 3. The figure shows (a) the 20 most discriminatory Euclidean distance features, and (b) the 20 most discriminatory geodesic distance features. Note that the geodesic distances are symbolically depicted by straight lines. In reality geodesics paths are along the facial surface.

For the existing 3D face recognition techniques based on

local facial features, rank one RR values ranging from 78% to 100% have been reported on data sets of varying sizes [11]. Higher recognition rates in general have been reported for data sets containing 3D models of relatively few subjects. However, the performances of these algorithms and ours are not directly comparable as they all have been evaluated on different data sets, using different different training and evaluation protocols. The rank 1 RR values attained by our proposed algorithms on our data set, however, were higher than that achieved by the 3D EBGM algorithm (rank 1 RR = 86.9%), on the FRGC data set of 466 subjects [14].

In conclusion, we have identified discriminatory facial structural characteristics from the literature on facial anthropometry and have developed effective 3D face recognition algorithms that incorporate them. We have empirically demonstrated the effectiveness of our proposed algorithms, their robustness to changes in facial expressions, and superior performance relative to algorithms that employ distances between arbitrary facial fiducial points. As a follow up to this analysis, we will investigate techniques to automatically locate anthropometric fiducial points. This would be the next logical step towards building a completely automatic 3D face recognition system based on discriminatory anthropometric facial measurements.

Acknowledgments

We would like to gratefully acknowledge Advanced Digital Imaging Research, LLC, Friendswood, TX for providing 3D facial data and financial support for this project.

References

[1] S. Belongie, J. Malik, and J. Puzicha. Shape matching and object recognition using shape contexts. *Pattern Analysis and Machine Intelligence, IEEE Transactions on*, 24(4):509–522, 2002.

[2] A. M. Bronstein, M. M. Bronstein, and R. Kimmel. Three-dimensional face recognition. *International Journal of Computer Vision*, 64(1):5–30, 2005.

[3] J. Comas. *Manual of Physical Anthropology*. Charles C. Thomas, 1960.

[4] D. DeCarlo, D. Metaxas, and M. Stone. An anthropometric face model using variational techniques. In *SIGGRAPH*, pages 67–74, 1998.

[5] E. W. Dijkstra. A note on two problems in connexion with graphs. *Numerische Mathematik*, 1:269–271, 1959.

[6] L. Farkas. *Anthropometric Facial Proportions in Medicine*. Thomas Books, 1987.

[7] L. G. Farkas. *Anthropometry of the Head and Face in Medicine*. Elsevier, New York, 1981.

[8] L. G. Farkas, M. I. R., and K. J. C. An attempt to define the attractive face: an anthropometric study. In *18th Annual meeting of the American Society for Aesthetic Plastic Surgery*, Boston, April 15 1985.

[9] G. G. Gordon. Face recognition based on depth and curvature features. In *Computer Vision and Pattern Recognition, 1992. Proceedings CVPR '92., 1992 IEEE Computer Society Conference on*, pages 808–810, 1992.

[10] S. Gupta, M. K. Markey, J. K. Aggarwal, and A. C. Bovik. 3d face recognition based on euclidean and geodesic distances. In *Electronic Imaging, IS&T/SPIE 19th Annual Symposium on*, San Jose, CA, January 2007.

[11] S. Gupta, M. K. Markey, and A. C. Bovik. *Pattern Recognition Research Horizons*, chapter Advances and Challenges in 3D and 2D+3D Human Face Recognition. Nova Science Publishers, Inc, New York, 2007.

[12] A. Hamza and H. Krim. Geodesic matching of triangulated surfaces. *Image Processing, IEEE Transactions on*, 15(8):2249–2258, 2006.

[13] A. Hrdlička. *Practical Anthropometry*. Wister Institute of Anatomy and Biology, Philadelphia, 1939.

[14] M. Hüsken, M. Brauckmann, S. Gehlen, and C. Von der Malsburg. Strategies and benefits of fusion of 2d and 3d face recognition. In *Computer Vision and Pattern Recognition, 2005 IEEE Computer Society Conference on*, volume 3, pages 174–174, 2005.

[15] Y. Lee, H. Song, U. Yang, H. Shin, and K. Sohn. Local feature based 3d face recognition. In *Audio- and Video-based Biometric Person Authentication, 2005 International Conference on, LNCS*, volume 3546, pages 909–918, 2005.

[16] D. Lowe. Distinctive image features from scale-invariant keypoints. *International Journal of Computer Vision*, 60(2):91–110, 2004.

[17] X. Lu, A. K. Jain, and D. Colbry. Matching 2.5d face scans to 3d models. *Pattern Analysis and Machine Intelligence, IEEE Transactions on*, 28(1):31–43, 2006.

[18] A. B. Moreno, A. Sanchez, J. Fco, V. Fco, and J. Diaz. Face recognition using 3d surface-extracted descriptors. In *Irish Machine Vision and Image Processing Conference (IMVIP 2003)*, Sepetember 2003.

[19] P. S. Penev and J. J. Atick. Local feature analysis: a general statistical theory for object representation. *Network: Computation in Neural Systems*, 7:477–500, 1996.

[20] P. J. Phillips, P. Grother, R. J. Micheals, D. M. Blackburn, E. Tabassi, and M. Bone. Face recognition vendor test 2002 evaluation report. Technical report, National Institute of Standards and Technology, 2003.

[21] B. O. Rogers. The role of physical anthropometry in plastic surgery today. *Clinical Plastic Surgery*, 1:439, 1974.

[22] J. B. Tenenbaum, V. de Silva, and J. C. Langford. A global geometric framework for nonlinear dimensionality reduction. *Science*, 290(5500):2319–2323, 2000.

[23] Y. Wang, C. Chua, and Y. Ho. Facial feature detection and face recognition from 2d and 3d images. *Pattern Recognition Letters*, 23(10):1191–1202, 2002.

[24] L. Wiskott, J.-M. Fellous, N. Kuiger, and C. von der Malsburg. Face recognition by elastic bunch graph matching. *Pattern Analysis and Machine Intelligence, IEEE Transactions on*, 19(7):775–779, 1997.